

Gas kinetic studies using a table-top set-up with electron beam excitation: quenching of molecular nitrogen emission by water vapour

A. Morozov¹, R. Krücken¹, J. Wieser², and A. Ulrich^{1,a}

¹ Fakultät für Physik E12, Technische Universität München, 85748 Garching, Germany

² TuiLaser, Industriestr. 15, 82110 Germering, Germany

Received 19 January 2005 / Received in final form 23 February 2005

Published online 26 April 2005 – © EDP Sciences, Società Italiana di Fisica, Springer-Verlag 2005

Abstract. A table-top set-up for studying gas kinetic processes in dense gases via time resolved optical spectroscopy is presented. The set-up uses low energy electron beams for gas excitation. A thin silicon nitride membrane separating the electron source and the gas cell allows to use electron energies as low as 10–15 keV. The electron source is operated in a fast pulsing mode with a pulse width of 5 ns and repetition rates up to 30 kHz. Light emission from the target gas sample is studied and time resolved photon counting is used to measure decay times and collisional rate constants for specific excited states. The experimental concept is applied to measure the rate constants for quenching of molecular nitrogen in the $C^3\Pi_u$ state (vibrational levels 0 and 1) by water vapour. Quenching rate constants of $(7.1 \pm 0.7) \times 10^{-10} \text{ s}^{-1} \text{ cm}^3$ and $(6.7 \pm 0.7) \times 10^{-10} \text{ s}^{-1} \text{ cm}^3$ were obtained for the $C^3\Pi_u (v = 0)$ and $C^3\Pi_u (v = 1)$ vibrational levels, respectively.

PACS. 34.80.Dp Atomic excitation and ionization by electron impact – 34.80.Gs Molecular excitation and ionization by electron impact – 33.50.Hv Radiationless transitions, quenching

1 Introduction

Gas kinetic studies are the key method for obtaining information on radiative properties of any excited gas medium. The studies provide data on excitation and deexcitation processes and the corresponding reaction rate constants. This information is vital for developing new or improving existing light sources or gas lasers. Many methods are currently applied in gas kinetic studies and the main difference lies in the excitation technique (e.g. electrical discharges, photo- or particle beam excitation) and in the technique which is used to detect the response of the medium. The advantages and disadvantages of the excitation technique used in a study often have critical effect on what information on a specific medium can be reliably obtained.

In this work we use short pulsed particle beam excitation of gas media which leads to population of excited states either via direct collisional excitation or subsequent gas kinetic reactions. Time resolved optical spectroscopy is used as the detection technique. Gas kinetic information is extracted from time spectra of light intensity using the fact that the time evolution of emission intensity follows the emitting specie's population density. It is often possible to extract information on the effective lifetimes of the emitting species at the selected conditions such as

pressure, mixing ratios etc., and, by varying these conditions, to obtain collisional rate constants. Gas kinetic studies based on this concept and using heavy ion beams have been presented in earlier publications [1–5].

Particle beam excitation has a number of important advantages. It allows a wide range of gas pressures, typically from essentially zero up to many times the atmospheric pressure, without ignition problems or arcing which limits the use of gas discharges. The maximum pressure is limited by the dimensions and the material of the window through which the beam is sent into the gas. There is no debris production due to electrode erosion, therefore very high gas purity can be maintained during experiments. This is especially important when studying gas media where small admixtures of impurities have a substantial effect on the gas kinetic processes. Since the exciting beam is formed outside of the gas volume, it is possible to precisely measure and control the temporal profile of the excitation pulse. Finally, the beam currents can normally be low enough not to alter the gas temperature, so that temperature dependencies can be studied using external heating or cooling of the gas to a well defined temperature.

However, high energy beam excitation has also a number of specific characteristics which may be often considered as disadvantages. The installations which provide such beams (e.g. ion or electron accelerators) are usually

^a e-mail: Andreas.Ulrich@ph.tum.de

very large and expensive, and using these facilities is quite complicated both technically and administratively. In some cases, when heavy projectiles with a high charge state are used it might be difficult to interpret emission data due to very effective multiple ionization processes. Radioactive sources, which belong to an alternative type of high energy particle sources, are compact, however their handling raises safety issues and the random nature of particle emission implies certain complications concerning triggering and detection.

In this paper, we introduce a method of using low energy electron beam excitation which avoids most of the problems described above but still has the advantages of particle beam excitation. This excitation technique was introduced in our previous papers on light sources [6–8]. The main novelty is the application of thin (300 nm) silicon nitride membranes to separate the electron beam source from the gas cell. These membranes allow for electron energies on the order of 10 keV. Such low electron energy has a number of important advantages over electron energies of 50 keV and more used in traditional techniques with metal membranes. First of all, this excitation can be realized in very compact, tabletop systems which do not produce hard X-rays. The low energy electron beams can be produced with simple electron guns. These electron guns work in both dc (direct current) and pulsed modes, with minimum pulse width as short as a few nanoseconds. Finally, the low energy of the projectiles gives short penetration depths in gas targets leading to high brightness [6] of the light emission.

The advantages of the low energy electron beam excitation make this technique a powerful tool for spectroscopic and, especially, gas kinetic studies of gases and gas mixtures. Since many technical improvements concerning the electron beam source, in particular the introduction of the fast pulsing mode, have been made from the time when the pioneering paper on the low energy electron beam technology [6] was published, we present a detailed description of the experimental set-up. In the present work the experimental concept was first applied to measure the radiative lifetimes of the molecular nitrogen state $C^3\Pi_u$ (vibrational levels 0 and 1) and the collisional self-quenching rate constants for these levels. Since the gas kinetic data on these levels are already well-known, this application is a good test of the experimental technique. Then the technique was used to measure quenching rate constants of molecular nitrogen by water vapour, which is not yet sufficiently studied.

There is renewed interest in nitrogen emission from ultrahigh-energy cosmic ray particle physics where so-called air showers are induced by the primary cosmic ray particle [9]. This field of research implies detection and analysis of the light emission from the atmosphere following each impact, in particular, emission from molecular nitrogen originating from transitions between the states $C^3\Pi_u$ and $B^3\Pi_g$ (the so called second positive system of nitrogen). To analyze the emission data, detailed information on nitrogen emission from air as a function of partial pressure of all its components should be known. According

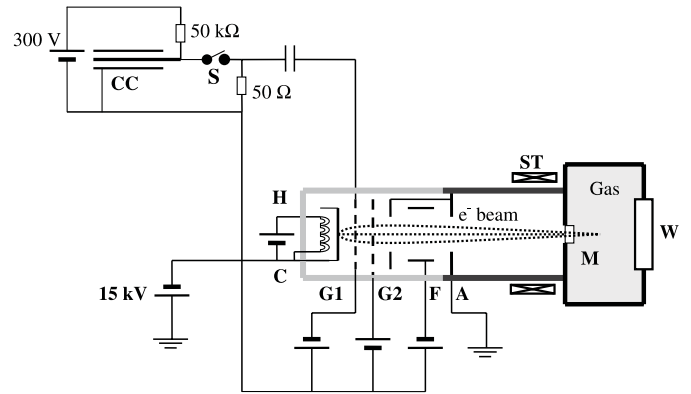


Fig. 1. Schematic drawing of the electron gun with the attached gas cell and the pulser unit. The anode **A** is on ground potential. All other electrodes are on high negative potential and have some offset voltage from the potential of the cathode **C**: The offset potential on the control grid **G1** is 0–100 V, on the extraction grid **G2** +600 V, and on the focusing electrode **F** 0–1000 V. The voltage on the heater **H** is 6–10 V. Magnetic steering **ST** is used to guide the electron beam through the membrane **M** into the gas cell with the attached window **W**. The pulser unit (top left corner) is powered by 300 V. A discharge of the coaxial cable **CC** (0.5 m, 50 Ohm impedance), initiated by the fast switch **S**, creates +110 V ~ 15 ns voltage pulses on **G1** leading to ~5 ns electron beam pulses.

to our knowledge, the effect of water vapour on nitrogen emission was not yet discussed in papers on air showers, probably because water vapour concentration in the atmospheric air is usually only about 1% at sea level and decreases with temperature and altitude. However, this effect might be significant since the collisional quenching rate constants for molecular nitrogen in the state $C^3\Pi_u$ ($v = 0, 1$) by water vapour, known from the literature, are about 30% larger [10] than the constants for quenching by oxygen and about 40 times [10] larger than the nitrogen self-quenching rate constants. The results presented in this paper show that the quenching rate constants of nitrogen by water vapour were previously underestimated nearly by a factor of two, which suggests that the effect of water vapour on the emission from nitrogen in air shower experiments should be carefully treated.

2 Experimental set-up

A commercially available electron gun (Clinton Electronics model 3-659) designed for monochrome displays was used to provide electron beams. A schematic drawing of the electron gun and related electrical circuits is shown in Figure 1. Typically, acceleration voltages from 10 to 15 kV were applied. The cathode of the electron gun was operated at high negative potential and the anode was connected to the ground. The gun was installed in a glass-metal chamber which was kept under a vacuum better than 5×10^{-6} hPa using a turbo molecular pump. A 2 mm diameter aperture in a CF40 flange separating the electron gun volume from the gas cell was covered with a

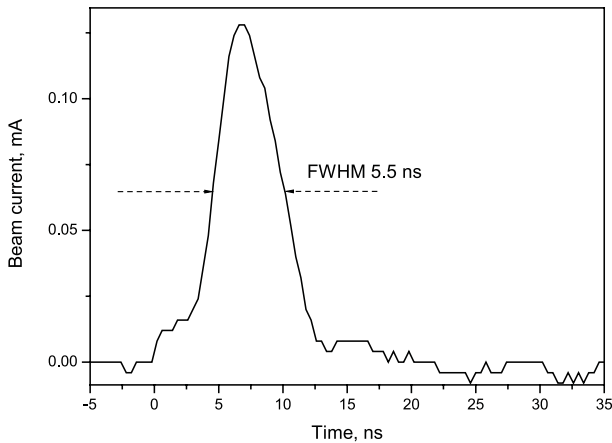


Fig. 2. Time evolution of an electron beam current during one pulse recorded with a faraday cup placed in the evacuated gas cell.

thin (300 nm) silicon nitride membrane ($0.7 \times 0.7 \text{ mm}^2$) on a $5 \times 5 \text{ mm}^2$ section of a silicon wafer. Energy loss of electrons in such membranes is about 8% for 20 keV electrons [6] and gradually increases with decreasing electron energy (15% at 15 keV, 40% at 10 keV, and 100% loss at 5 keV). Such membranes can withstand pressure differentials up to typically ten bars and an average beam current density of about $40 \mu\text{A}/\text{mm}^2$. More membrane-related issues were presented in [6]. One of the electrodes of the electron gun allows focusing of the electron beam and two pairs of external magnetic coils are used to steer the electron beam through the membrane.

Pulsing of the electron beam was performed using the control grid of the electron gun. Application of a negative voltage of about 100 V to that grid with respect to cathode potential stops the electron beam completely. Keeping that offset voltage and applying fast positive (on the order of 100 V) pulses to the same grid produces short electron beam pulses. The positive pulses were formed using a device known as “cable pulser” (see Fig. 1). The fast switch of the cable pulser is a commercially available device (Behlke model HTS 31) which provides up to 30 kV decoupling between the trigger input and the switch itself. This option was used to trigger the pulses from ground potential using a digital pulse generator (Stanford Research model DG535). A time evolution of the electron beam current during one pulse recorded with a faraday cup placed in the evacuated gas cell is shown in Figure 2. This time dependence of the beam current was recorded using a digital storage oscilloscope (Tektronics model 2440).

The gas cell was attached to the flange where the silicon nitride membrane was installed. The cell was a stainless steel cylinder of 3 cm inner diameter and 5 cm length. The inner walls of the cell have been covered with a thin layer of gold to minimize impurity release due to scattered electrons and ultraviolet radiation. Continuous irradiation of nitrogen in the cell and repeated measurements of a decay rate has shown that impurity production is negligible for all exposure times used in this work. The original purity of nitrogen used in this study was 99.999%. The nitro-

gen pressure was monitored using a capacitive manometer (MKS Baratron 690A) temperature controlled to 45°C . The manometer has an accuracy of 0.12% of the reading and an uncertainty of 0.02 hPa due to zero drift with temperature. To prepare nitrogen water-vapour mixtures, the evacuated gas cell was first filled with water vapour from a special volume containing bi-distilled and degassed water and then nitrogen was added. Partial pressure of water vapour was monitored during the experiments using an impedance dewpoint hygrometer (“Easidew Transmitter” from Michel Instruments) which was installed in a side branch of the cell. The hygrometer shows repeatability of water vapour pressure reading of about 10%. The hygrometer was calibrated using the capacitive manometer, which, according to the manufacturer can reliably measure water vapour pressures. During electron beam irradiation of gas mixtures no change in hygrometer reading was observed at any water vapour pressure.

Light emission from the electron beam excited gas was observed through a MgF_2 window which is transparent over a wide spectral range starting from the short-wavelength cut-off at about 120 nm. Spectral observations were performed using a vacuum monochromator (McPherson model 218) with 30 cm focal length. This monochromator offers a wavelength range from 105 nm to 60 μm (several interchangeable gratings) and has a maximum wavelength resolution of 0.03 nm. The monochromator was equipped with a 50 mm diameter photo multiplier tube with a MgF_2 entrance window and a S20 photocathode, which limits the wavelength range to 120–800 nm. The PM tube was operated in the photon counting mode. To avoid pile-up effects (distortion of time spectra due to the fact that if several photons arrive during one pulse only the earliest one will be recorded), the light output of the source was adjusted in such a way that less than one photon per ten triggering pulses (averaged) was registered by the PM tube.

The time delay between a trigger pulse which starts the cable pulser and a photomultiplier pulse from a detected photon was measured with a time-to-amplitude converter (Ortec model 566). The available full-range setting of the converter module ranges from 50 ns to 100 μs . The output signal of the module has an amplitude proportional to the time difference between the start and stop pulses. The amplitude was analyzed with a 13 bit analog-to-digital converter (Ortec model AD413A). Data were transferred to a PC computer using a CAMAC-to-PC interface controller (Wiener model CC32). The electronic time resolution of the data acquisition system was better than 0.6 ns when the time-to-amplitude converter was operating at a full scale setting of 1000 ns.

3 Nitrogen $C^3\Pi_u$ state: collisional self-quenching and radiative lifetimes

As the first application of the novel experimental set-up described above, radiative lifetimes and collisional quenching rates were measured for the first two vibrational levels of the molecular nitrogen state $C^3\Pi_u$.

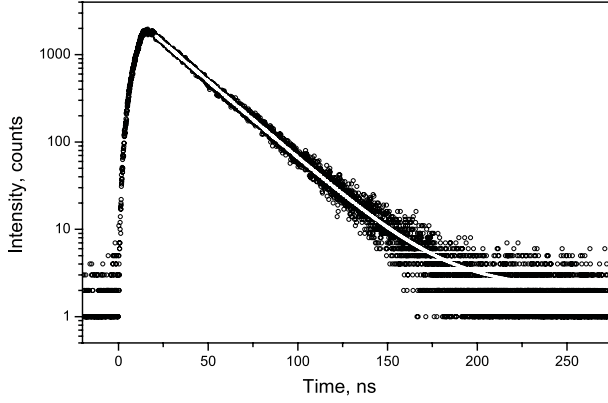


Fig. 3. Time evolution of light emission from 50 hPa nitrogen recorded at the 337 nm transition. Hollow dots show experimental points. The white straight line through the data points is a numerical fit (exponential decay plus background).

An example of a time spectrum recorded for the emission band at 337 nm ($v' = 0 \rightarrow v'' = 0$) is shown in Figure 3. One million photons were counted to record this spectrum. The wavelength resolution of 1 nm (used for all spectra recorded in this study) assures that the time spectrum measured at the central wavelength of each band contains emission only from this band. As it can be seen from Figure 3, the decay part of the curve is exponential with a very low intensity background. In the same figure the solid line shows fitting of the experimental data with the function:

$$I(t) = I_0 + Me^{-R(t-t_0)}, \quad (1)$$

where R is the total decay rate of the upper state, I_0 is the background intensity and M is the intensity at the time t_0 (corrected for the background). Time spectra recorded with the full time scale of 100 μ s have shown that light emission ends completely after a few hundred nanoseconds after the excitation pulse. The background intensity, which is approximately three orders of magnitude lower than the peak intensity, does not increase when the repetition rate is gradually increased up to the maximum rate of 30 kHz. This indicates that all excited species decay completely before the next excitation pulse is applied.

To determine the radiative lifetimes τ and the collisional quenching rate coefficients Q_{N_2} for the two lowest vibrational levels of the molecular nitrogen state $C^3\Pi_u$, time spectra of two molecular bands were recorded at various pressures of nitrogen P_{N_2} and the exponential decay rate R of emission intensity was derived from the experimental data according to equation (1). Since the total decay rate is a combination of the radiative decay and collisional quenching:

$$R = 1/\tau + Q_{N_2} \times P_{N_2}, \quad (2)$$

the radiative lifetime can be found from extrapolation of the decay rate to zero pressure and the quenching rate from the slope of the decay rate versus pressure. This procedure was applied for the N_2 band at 337 nm

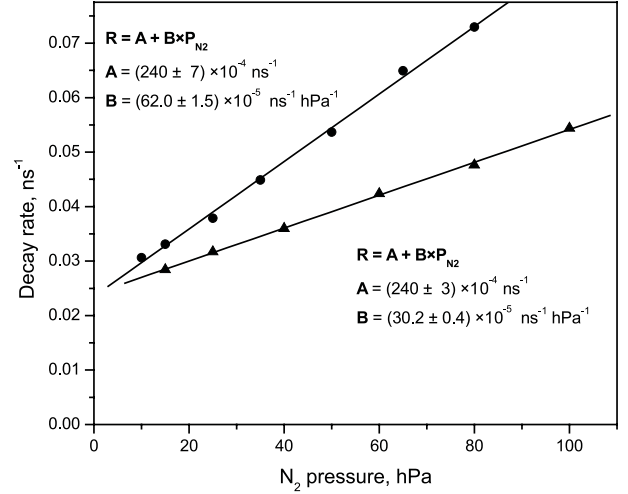


Fig. 4. Pressure dependences of the decay rate of the molecular nitrogen state $C^3\Pi_u$ (triangular dots for the emission from $v = 0$ and round dots for the emission from $v = 1$). Data points and linear fits (solid lines) are shown. The values of the fitting parameters A and B are shown for the vibrational levels 0 and 1 on the lower right and on the upper left side, respectively.

($v' = 0 \rightarrow v'' = 0$ transition) and for the band at 316 nm ($v' = 1 \rightarrow v'' = 0$ transition). The pressure dependences of decay rates for the bands are shown in Figure 4. Linear fits according to equation (2) result in the following values for lifetimes τ and collisional quenching rate coefficients Q_{N_2} for the $N_2 C^3\Pi_u$ state:

- vibrational level 0: $\tau = 41.7 \pm 1.4$ ns,
 $Q_{N_2} = (3.0 \pm 0.2) \times 10^5 \text{ s}^{-1} \text{ hPa}^{-1}$
 $\rightarrow (1.2 \pm 0.1) \times 10^{-11} \text{ s}^{-1} \text{ cm}^3$;
- vibrational level 1: $\tau = 41.7 \pm 2.1$ ns,
 $Q_{N_2} = (6.2 \pm 0.2) \times 10^5 \text{ s}^{-1} \text{ hPa}^{-1}$
 $\rightarrow (2.5 \pm 0.1) \times 10^{-11} \text{ s}^{-1} \text{ cm}^3$.

The pressure to density conversion is done using the gas temperature of 293 K. The obtained lifetimes and quenching rate coefficients are in a very good agreement with published data (see [10,11] and references therein) which, on one hand, confirms these values using an alternative experimental approach and on the other hand provides a reliable verification for the presented experimental technique.

4 Quenching of nitrogen $C^3\Pi_u$ state by water vapour

A technique similar to the one described in Section 3 was applied to measure quenching rates of molecular nitrogen in the $C^3\Pi_u$ state by water vapour. For nitrogen water-vapour mixtures the decay rate R of the emission (see Eq. (2) for the pure nitrogen case) is proportional to the

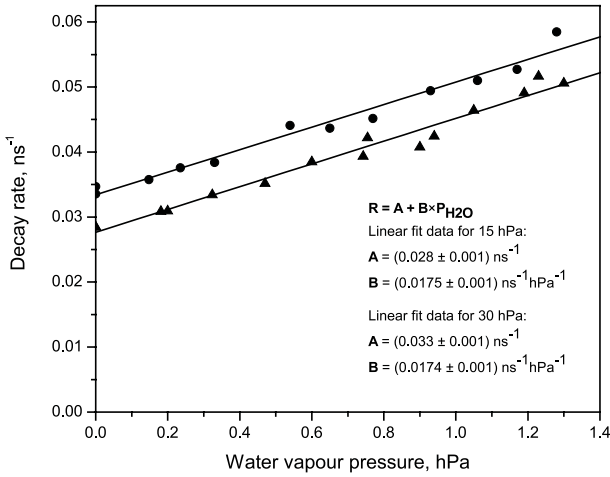


Fig. 5. Pressure dependence of the decay rate of the molecular nitrogen state C^3I_u ($\nu = 0$) in nitrogen water-vapour mixtures. Round and triangular dots show the results for mixtures with 30 hPa and 15 hPa nitrogen pressure, respectively. Linear fits (solid lines) as well as A and B parameter values are also shown.

partial water vapour pressure P_{H_2O} :

$$R = 1/\tau + Q_{N_2} \times P_{N_2} + Q_{H_2O} \times P_{H_2O}. \quad (3)$$

Decay rates of emission from vibrational levels 0 and 1 were recorded using gas mixtures at a fixed nitrogen pressure and different water vapour partial pressures. The decay rates and results of the linear fit for vibrational level 0 (337 nm band) and level 1 (316 nm band) are shown in Figures 5 and 6, respectively. The data result in the following quenching rate coefficients Q_{H_2O} :

- vibrational level 0:

$$(17.5 \pm 1.8) \times 10^6 \text{ s}^{-1} \text{ hPa}^{-1} \\ \rightarrow (7.1 \pm 0.7) \times 10^{-10} \text{ s}^{-1} \text{ cm}^3$$

- vibrational level 1:

$$(16.5 \pm 1.7) \times 10^6 \text{ s}^{-1} \text{ hPa}^{-1} \\ \rightarrow (6.7 \pm 0.7) \times 10^{-10} \text{ s}^{-1} \text{ cm}^3.$$

The values of the coefficients obtained in this work are about two times larger than data which can be found in the literature. There are two papers [10,12] where the quenching of nitrogen emission by water vapour has been studied. However, the values given in the reference [12] have large uncertainties (up to 40%) and it is not described how the nitrogen water-vapour mixtures were prepared and how water vapour pressure was monitored except for a sentence that water content was measured by an ionization hygrometer. In reference [10] the water vapour pressure was derived from the assumption that hydrogen and oxygen which were added as admixtures to nitrogen were completely converted to water vapour in the cell due to gas excitation. If this assumption was not valid, the actual water vapour pressure might have been lower than expected, which, in turn, would result in values of the quenching rate coefficients which are lower than actual.

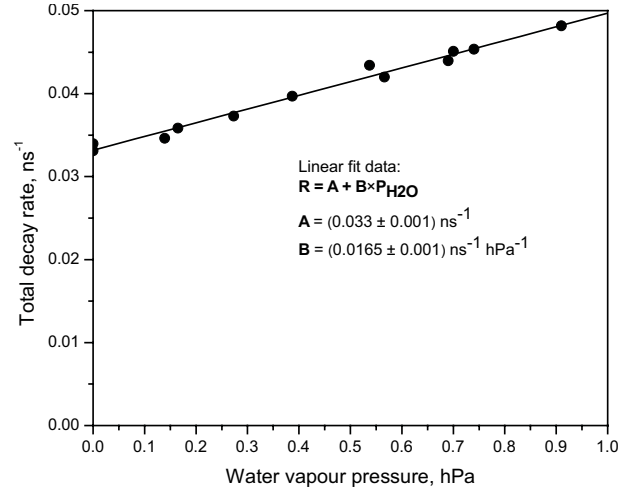


Fig. 6. Pressure dependence of the decay rate of the molecular nitrogen state C^3I_u ($\nu = 1$) in nitrogen–water vapour mixtures. The nitrogen pressure is 15 hPa. Linear fits (solid lines) as well as A and B parameter values are also shown.

Another possibility is that a part of the water molecules created in the cell was attached to the gas cell walls. In the present work, to avoid similar uncertainties with the actual content of the water in the gas phase, the partial pressure of water vapour was continuously monitored during the experiments.

The authors thank Hans Klages and Paolo Privitera for introducing them to the research field of air showers physics. The authors gratefully acknowledge the Bayerische Forschungsgesellschaft for funding the research project (grant 482/01) and the Maier-Leibnitz-Laboratorium München for financial support.

References

1. W. Krötz, A. Ulrich, B. Busch, G. Ribitzki, J. Wieser, Appl. Phys. Lett. **55**, 2265 (1989)
2. W. Krötz, A. Ulrich, B. Busch, G. Ribitzki, J. Wieser, Phys. Rev. A **43**, 6089 (1991)
3. W. Krötz, A. Ulrich, G. Ribitzki, J. Wieser, D.E. Murnick, Hyperf. Interact. **88**, 193 (1994)
4. A. Ulrich, R. Gernhäuser, W. Krötz, J. Wieser, D.E. Murnick, Phys. Rev. A **50**, 1931 (1994)
5. G. Ribitzki, A. Ulrich, B. Busch, W. Krötz, J. Wieser, D.E. Murnick, Phys. Rev. E **50**, 3973 (1994)
6. J. Wieser, D.E. Murnick, A. Ulrich, H.A. Huggins, A. Liddle, W.L. Brown, Rev. Sci. Instrum. **68**, 1360 (1997)
7. J. Wieser, M. Salvermoser, L.H. Shaw, A. Ulrich, D.E. Murnick, H. Dahi, J. Phys. B: At. Mol. Opt. Phys. **31**, 4589 (1998)
8. A. Ulrich, C. Niessl, J. Wieser, H. Tomizawa, D.E. Murnick, M. Salvermoser, J. Appl. Phys. **86**, 3525 (1999)
9. M. Nagano, K. Kobayakawa, N. Sakaki, K. Ando, Astroparticle Phys. **20**, 293 (2003)
10. S.V. Pancheshnyi, S.M. Starikovskaia, A.Yu. Starikovskii, Chem. Phys. **262**, 349 (2000)
11. M. Simek, S. DeBenedictis, G. Dilecce, V. Babický, M. Clupek, P. Sunka, J. Phys. D: Appl. Phys. **35**, 1981 (2002)
12. F. Albugues, A. Birot, D. Blanc, H. Brunet, J. Galy, P. Millet, J.L. Teyssier, J. Chem. Phys. **61**, 2695 (1974)